Journal of Biomechanics 46 (2013) 931–940

Contents lists available at SciVerse ScienceDirect

Journal of Biomechanics

journal homepage: www.elsevier.com/locate/jbiomech
www.JBiomech.com

Biomechanical properties and histological structure of sinus of Valsalva aneurysms in relation to age and region

Dimitrios C. Iliopoulos [a,b], Eleftherios P. Kritharis [c], Spyridon Boussias [b], Alexandros Demis [b], Christos D. Iliopoulos [b], Dimitrios P. Sokolis [c,*]

[a] Laboratory of Experimental Surgery and Surgical Research, School of Medicine, University of Athens, Athens, Greece
[b] Department of Cardiothoracic Surgery, Athens Medical Center, Athens, Greece
[c] Laboratory of Biomechanics, Center of Experimental Surgery, Biomedical Research Foundation of the Academy of Athens, Athens, Greece

ARTICLE INFO

Article history:
Accepted 13 December 2012

Keywords:
Aortic sinus
Uniaxial tension
Quantitative histology
Strain–energy function
Anisotropy.

ABSTRACT

Information on the biomechanical properties of aortic root aneurysms that would facilitate our understanding of their rupture modes is currently unavailable. In this study, whole-thickness wall specimens from aortic root aneurysms were studied *in vitro* so as to compare the biomechanical properties with gross histomorphology and composition, in relation to age, region, and direction. The stress–strain relationship was determined under uniaxial loading conditions and characterized by the Fung-type material model in terms of optimized material constants; failure properties were recorded. The connective tissue contents of the basic scleroproteins were also determined through computerized histology. Aging had a deleterious influence on the tensile strength of the aneurysmal sinus tissue, causing also stiffening and reduced extensibility that was consistent with the deficient elastin and collagen contents. Direction-dependent differences were demonstrated in the noncoronary sinus, with the circumferential being stiffer and stronger than the longitudinal direction, justified by the preferred collagen reinforcement along that direction there. In the left and right coronary sinus, the material constants and failure properties were essentially the same in the two directions, justified by the arbitrary orientation of medial (collagen and elastin fibers, and cellular) components relative to the circumferential–longitudinal directions. The material characterization results afforded, and the regional and age-related differences in the strength of the sinus wall, i.e. in its capacity to withstand hemodynamic stresses, are hoped to provide novel insight into the pathophysiological mechanisms responsible for the highest incidence of ruptured aortic root aneurysms in the right coronary and noncoronary sinus.

1. Introduction

An aortic aneurysm represents a pathological dilation of the vessel which is greater than 1.5 times its normal size (Svensson and Crawford, 1997). It typically develops at sites with an underlying weakness in the medial layer of the aortic wall; susceptible sites associated with congenital or acquired conditions. Once begun, aneurysm formation is promoted by biomechanical laws and eventual rupture may be expected when the aortic wall strength is overcome by the hemodynamic stresses acting on the vessel (Vorp, 2007). Depending on the site of occurrence, aortic aneurysms are classified into aortic root or sinus of Valsalva aneurysms, thoracic, and abdominal aortic aneurysms. Compared to the latter two types, which are more frequent and tend to manifest themselves during the 5th–7th decades of life, sinus of Valsalva aneurysms arise rarely. Their incidence is 0.14–0.96% in patients undergoing open heart surgery (Takach et al., 1999) and frequently concern patients in their 2nd–4th decades of life (David, 2010). Among their detrimental consequences are aortic insufficiency, dissection, and rupture. Current guidelines recommend surgical intervention when aneurysm diameter exceeds 50 mm, but surgery may occasionally be indicated at smaller diameters.

Given the biomechanical nature of the dissection/rupture of aortic root aneurysms, the need for biomechanical analysis is clear. In contrast to thoracic and abdominal aortic aneurysms, for which there have been a number of previous communications (see (Vorp, 2007; Phillippi et al., 2011; Sokolis et al., 2012; Humphrey and Holzapfel, 2012) and references therein), no information exists about the aneurysmal aortic root, perhaps because of their relative paucity. Little is known about healthy sinuses and the results are conflicting (Ferraresi et al., 1999;

* Correspondence to: 35, Lefkados Street, Athens 15354, Greece. Tel.: +30 210 6597370; fax: +30 210 6597365.
E-mail address: DimitrisSokolis@ath.forthnet.gr (D.P. Sokolis).

0021-9290/$ - see front matter © 2012 Elsevier Ltd. All rights reserved.
http://dx.doi.org/10.1016/j.jbiomech.2012.12.004

Gundiah et al., 2008a,b; Martin et al., 2011). Our objective was to compare the basic failure properties and material constants characterizing the stress–stretch response of aneurysmal left (LCS), right (RCS), and noncoronary sinus (NCS), together with the effect of advanced age upon those properties. We also study by histomorphometric methods the connective tissue composition and arrangement of the main fibrous and cellular elements that underlie the biomechanical modification of dilated sinus wall.

2. Material and methods

2.1. Patients and specimen preparation

Between May 2007 and March 2012, aneurysmal aortic sinus tissue was procured from a series of 13 patients (age: 51 ± 6 years, diameter: 53 ± 17 mm, males: 8) during elective surgery at the Department of Cardiothoracic Surgery of Athens Medical Center, under informed consent following local ethical guidelines.

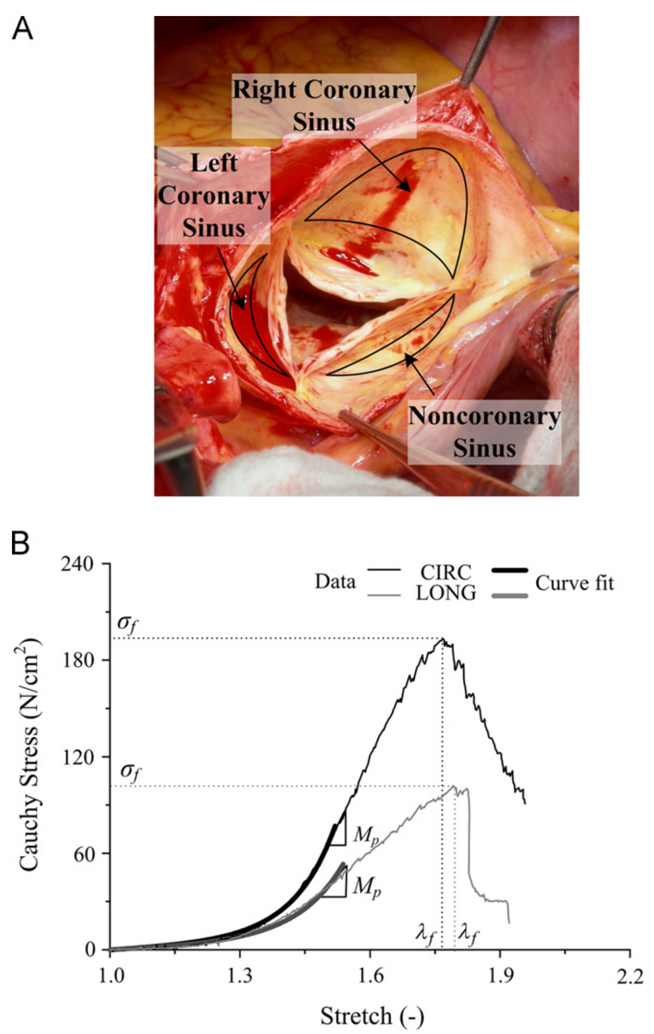

Fig. 1. (A) Aortic root aneurysm of a 67-year old patient undergoing elective surgery. The left (LCS), right (RCS), and noncoronary sinuses (NCS) are shown between thick lines. Tissue strips with CIRC and LONG orientation were harvested from these regions for histological analysis and biomechanical testing. (B) The diagram shows typical Cauchy stress vs. stretch curves of CIRC and LONG strips from the aneurysmal NCS wall. The parameters of failure stress σ_f (i.e. wall strength) and failure stretch λ_f (i.e. wall extensibility) are marked with dotted lines, and the slope is shown with a triangle that was used for the calculation of the peak elastic moduli M_p (i.e. maximum wall stiffness). The theoretical curves (Fung-type SEF predictions of Eq. (1)) are also plotted with thick lines, according to material constants $K=1.167$ N/cm², $c_{\theta\theta}=8.187$, $c_{zz}=7.185$, $c_{\theta z}=3.513$.

Table 1
Material constants of the Fung-type SEF and goodness of fit to the stress–strain data of LCS, RCS, and NCS tissue from young and old patients.

	Region	K (N/cm²)	$c_{\theta\theta}$ (−)	c_{zz} (−)	$c_{\theta z}$ (−)	ε (−)	r^2 (−)	λ_θ^{max} (−)	$\sqrt{2c_{zz}/c_{\theta z}+1}$ (−)	λ_z^{max} (−)	$\sqrt{2c_{\theta\theta}/c_{\theta z}+1}$ (−)
Young Patients	LCS ($n=4$)	4.152 ± 1.088	1.961 ± 0.583	1.880 ± 0.739	1.073 ± 0.502	3.674 ± 0.599	0.996 ± 0.001	1.663 ± 0.102	2.203 ± 0.075	1.730 ± 0.096	2.655 ± 0.570
	RCS ($n=5$)	$6.749\pm2.418^{\dagger}$	$1.415\pm0.673^{\dagger}$	$1.975\pm0.808^{\dagger}$	$1.059\pm0.471^{\dagger}$	3.817 ± 1.238	0.990 ± 0.004	1.764 ± 0.086	2.283 ± 0.167	1.631 ± 0.059	1.877 ± 0.095
	NCS ($n=8$)	$4.125\pm0.655^{\dagger}$	$2.106\pm0.277^{*\dagger}$	$1.789\pm0.249^{\dagger}$	$1.131\pm0.252^{\dagger}$	3.248 ± 0.831	0.993 ± 0.003	1.673 ± 0.045	1.973 ± 0.122	1.712 ± 0.060	2.110 ± 0.126
Old Patients	LCS ($n=6$)	1.599 ± 0.822	4.859 ± 1.602	3.958 ± 0.895	2.360 ± 0.667	2.358 ± 0.468	0.971 ± 0.015	1.409 ± 0.067	2.209 ± 0.286	1.382 ± 0.058	2.325 ± 0.312
	RCS ($n=12$)	2.041 ± 0.441	7.813 ± 1.774	5.490 ± 1.265	3.187 ± 0.680	4.692 ± 1.551	0.985 ± 0.004	1.404 ± 0.044	2.074 ± 0.068	1.424 ± 0.055	2.301 ± 0.131
	NCS ($n=16$)	1.209 ± 0.172	$7.703\pm1.685^{*}$	4.896 ± 0.638	3.873 ± 0.911	4.552 ± 1.153	0.987 ± 0.004	1.407 ± 0.038	2.073 ± 0.116	1.414 ± 0.051	2.377 ± 0.133

Constants are Mean ± SE. Refer to Eq. (5) in the text for the definitions of the root-mean-square error ε and the determination coefficient r^2.
$^{*}=p<0.05$ against c_{zz}
$^{\dagger}=p<0.05$ against old. n is the number of paired strips (i.e. one CIRC and one LONG strip), λ_θ^{max} and λ_z^{max} are the maximum stretch values used for material characterization in CIRC and LONG strips, respectively, and $\sqrt{2c_{zz}/c_{\theta z}+1}$ and $\sqrt{2c_{\theta\theta}/c_{\theta z}+1}$ the upper stretch bounds in Eq. (4).